PROCEEDINGS REPRINT

SPIE–The International Society for Optical Engineering



*Reprinted from*

# *Ultrafast Pulse Generation and Spectroscopy*

**18–19, 22 January 1993**
**Los Angeles, California**



**Volume 1861**





# Generation, measurement, and amplification of 20-fs high-peak-power pulses from a regeneratively initiated self-mode-locked Ti:sapphire laser

C. P. J. Barty, B. E. Lemoff and C. L. Gordon III

Edward L. Ginzton Laboratory, Stanford University, Stanford, California 94305

## ABSTRACT

We report the generation and measurement of 804 nm pulses with durations as short as 20 fs and with peak powers as high as 500 kW from a regeneratively initiated, self-mode-locked Ti:sapphire laser. Pulse duration is shown to decrease, and spectral content to increase, as intracavity power is increased. Control of intracavity focusing and a high-modulation-depth, acousto-optic modulator allow the intracavity power to be maximized. Cavity cubic phase error is minimized by correct design and placement of a GDD compensating prism pair. Methods for accurate determination of the pulse duration without assumption of pulse shape are discussed. Interferometric autocorrelation is accomplished with an interferometer which intrinsically balances dispersion and loss in each arm. Techniques for eliminating pulse distortions during amplification are also presented.

## 1. INTRODUCTION

Recently, there has been much interest in the generation of ultrashort pulses from mode-locked solid state lasers. Many groups have constructed oscillators capable of producing pulses of less than 50 fs in duration.[1-12] In this paper, we present a two-fold approach to the generation of short pulses in which we minimize cubic phase error in the laser cavity by correct design and placement of intracavity prisms and increase the phase-locked spectral content of the laser pulse by systematically raising the intracavity pulse power. This approach has resulted in pulses as short as 20 fs and peak pulse powers as high as 500 kW at 100-MHz repetition rate. Such pulses may be useful for the study of nonlinear phenomena or as high energy seed pulses for amplification systems.

The measurement of pulses with durations on the order of 20 fs presents several difficulties. Autocorrelation methods require knowledge of the temporal pulse shape for accuracy. However at such short pulse durations the common assumption of $\mathrm{sech}^2(t)$ pulse shape is often not valid. We use an accurate measurement of the spectral content of the pulse to determine the transform limited pulse shape and duration. In addition, systematic errors in the measurement device must be eliminated. We use an autocorrelator which intrinsically balances loss and group delay dispersion in each arm of its interferometer and which utilizes a thin (~50-μm) KDP crystal for second harmonic generation.



0-8194-1088-8/93/$6.00

Amplification of 20-fs pulses to several terawatts requires careful attention to linear and nonlinear pulse distortions. In order to avoid self-focusing and self-phase-modulation in the amplifiers, chirped pulse amplification is used.[13] Central to this technique is the ability to temporally stretch a seed pulse, amplify, and recompress without phase distortion. We have designed a 10,000 times stretching and compression system which is limited by quintic phase errors and should allow the production of 20–fs, 5-TW pulses. Pulse distortions due to refractive telescopes in typical amplification systems yield errors on the order of the pulse duration and have been eliminated from the current design through the use of reflective optics. Nonlinear pulse distortion after compression due to the nonlinear index of air has been avoided by enclosing the pulse compressor and subsequent experiments in vacuum chambers.

## 2. 20-FS TI:SAPPHIRE OSCILLATOR

### 2.1 Regeneratively initiated, self-modelocking

A schematic of our laser oscillator is shown in Fig. 1. The intracavity focusing mirrors, 2 cm Ti:sapphire rod, and rod housing are taken from a commercial cw Ti:Sapphire laser (Spectra Physics Model 3900). The laser is pumped by the all lines output of an argon ion laser (Spectra Physics Model 2040E) operating with between 7 and 20 watts of total optical power. The position of one focusing mirror is micrometer controlled and allows for the adjustment of overall intracavity focusing without affecting cavity alignment or dispersion. This adjustment is critical since mode locking is strongly dependent upon the spatial properties of the cavity mode inside the laser rod.

The two physical processes responsible for the generation of short pulses in our cavity are self-focusing and self-phase-modulation in the laser rod. When the cavity is properly aligned, an increase in self-focusing will lead to an increase in pump overlap, and hence a higher round trip gain for pulsed operation. This has the same effect as a fast saturable absorber.[10, 14] The extent to which the mode-locked (~$TEM_{00}$) and cw (~$TEM_{02}$) spatial modes differ for our laser is shown in Fig. 2. The cavity alignment is identical in the two cases. The pulse spectral content is further increased by self-phase-modulation in the laser rod. To the extent that this spectral content is phase-locked in a compressible manner, we expect the pulse duration to decrease as we increase the intracavity power.

Self-mode-locking is initiated by a regeneratively driven,[15, 16] intracavity acousto-optic modulator (AOM) (Brimrose Model FSML-4.4-2-C*). A portion of the output from the laser is incident upon a photodiode. Under cw operation, axial modebeating produces a ~100-MHz component at the photodiode which is then filtered, divided by 2, passed through a variable phase delay, amplified and used to drive the AOM. At 5 W of rf power, our AOM has a minimum modulation depth of 20% over a continuous range of modulation frequencies from 70 MHz to 110 MHz. This high nonresonant modulation depth not only

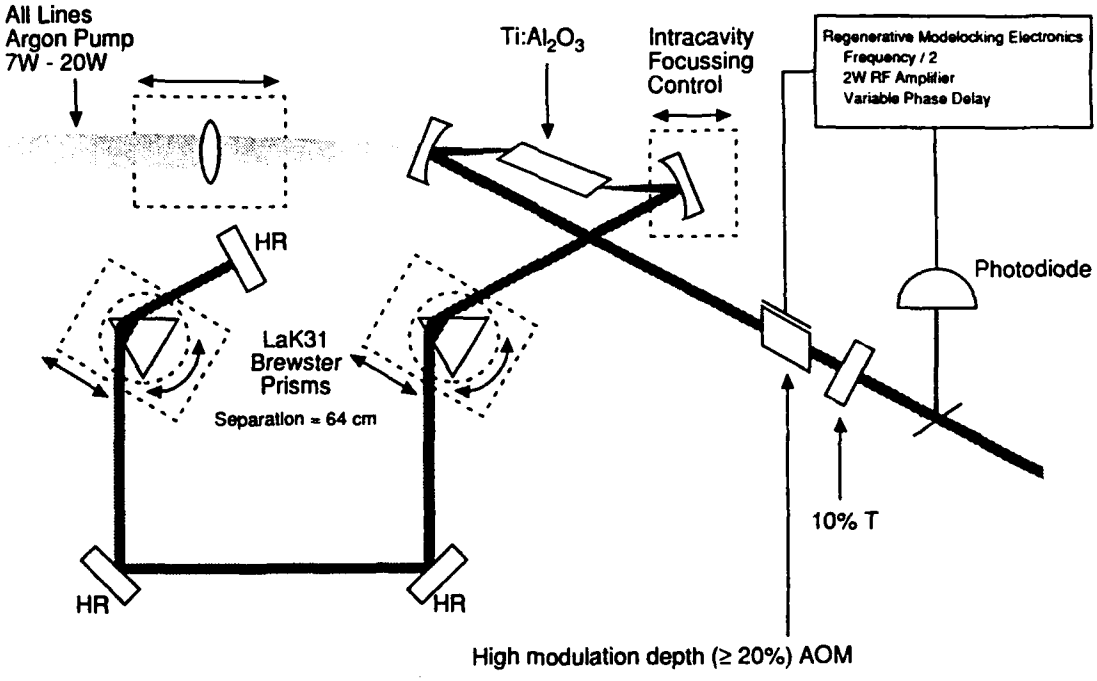


Figure 1. Schematic of the regeneratively initiated Ti:sapphire oscillator

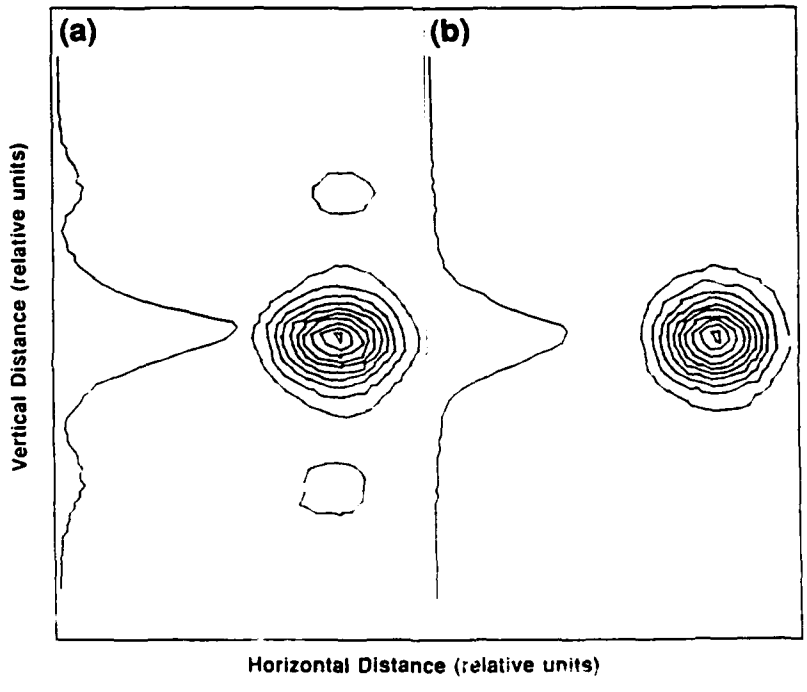


Figure 2. Far-field beam profiles of the laser output: (a) cw, (b) mode locked

provides the initial perturbation required for self-mode-locking to begin, but also helps to suppress concurrent cw modes that develop under highest power operation. This latter effect is confirmed by the observation that, when the AOM is turned off, one or more narrow lines appear over the otherwise unchanged pulse spectrum. By regeneratively driving the AOM, one avoids the need to accurately match the cavity length and thus round trip time to a fixed rf frequency.

2.2 Reduction of cavity cubic phase errors

An important consideration for short pulse oscillators is the control of pulse broadening due to uncompensated dispersion in the laser cavity. To understand this distortion, consider the Taylor series expansion of pulse delay, $\tau$, as a function of pulse carrier frequency given in Eq. 1. We may consider any

$$\tau(\omega) = \left.\frac{d\phi}{d\omega}\right|_{\omega_0} + (\omega-\omega_0)\left.\frac{d^2\phi}{d\omega^2}\right|_{\omega_0} + \frac{1}{2}(\omega-\omega_0)^2\left.\frac{d^3\phi}{d\omega^3}\right|_{\omega_0} + \frac{1}{6}(\omega-\omega_0)^3\left.\frac{d^4\phi}{d\omega^4}\right|_{\omega_0} \cdots \qquad \text{Eq. 1}$$

short pulse to be composed of longer duration pulses of different frequency and amplitude. An estimate of the pulse broadening on one round trip of the laser cavity may then be obtained by considering the delay of two pulses with carrier $\omega_0$ and $\omega_0+\Delta\omega/2$. In general, an intracavity prism pair is used to compensate for the large positive group delay dispersion (GDD), $d^2\phi/d\omega^2$, of the laser material and intracavity AOM. However, for pulses shorter than ~ 50 fs, higher order terms in the Taylor expansion become important. In particular, the cubic phase error ($d^3\phi/d\omega^3$) of the laser cavity may limit the pulse duration.[5, 17-21] The net dispersion of a prism pair is determined by the composition, apex angle, angle of incidence, intraprism path length, and interprism separation. We use a dispersive ray-tracing analysis to exactly calculate the effects of all of these parameters on all orders of dispersion. To minimize intracavity loss, the apex angle is chosen such that the central wavelength enters and exits the prisms at Brewster's angle. For a desired amount of negative GDD, the interprism separation is then determined by the prism composition and the intraprism path length. If we choose the prism pair GDD to exactly cancel the round trip GDD of the other cavity elements, the net round trip dispersive error of the cavity is dominated by the cubic phase term.

In Fig. 3, we show the round trip, cubic phase error, at 800 nm, as a function of prism composition and single pass, intraprism path length, for a net zero GVD cavity consisting of a 2 cm sapphire rod and a prism pair. From Fig. 3, we see that cavity cubic phase error is minimized for most of the materials shown when the beam passes as closely as possible to the prism apices (typical cavity beams require ~2 mm of prism insertion). This effect is especially pronounced in SF10. Experimentally, with SF10 prisms (no AOM in the cavity, prism separation of 22 cm, intraprism path length < 4 mm), we have been able to generate pulses as short as 26 fs. It should also be clear from Fig. 3 that minimizing intraprism path length does not always minimize cubic phase error. For BeO,[22] there is actually a finite

intraprism path length that simultaneously nulls GDD and cubic phase. Unfortunately, optical quality BeO is not a commercially available material. The next best choice of material would be fused silica; however, the interprism separation required to compensate for our rod and AOM (12 mm silica) is 143 cm. This separation is too large to allow stable mode formation with the intracavity elements shown in Fig. 1. We use LaK31 prisms, the required separation being only 50 cm. This yields a residual cubic phase error that is 60% less than a cavity with SF10 prisms.

2.3 Elimination of cavity cubic phase errors

There are some additional conclusions that can be drawn from ray tracing studies of the cavity phase errors. For most prism materials and laser operation at 800 nm one may reduce the cavity cubic phase simply by reducing the amount of bulk material in the laser cavity. This reduces the prism separation necessary to achieve a given amount of negative GDD and thus the amount of residual negative cubic phase from the prism pair. As an additional consequence, less dispersive prism materials with smaller cubic phase errors may be used without resulting in unstable cavity configurations. By going to a 4 mm laser rod, no intracavity AOM and silica prisms, one could reduce the cavity cubic phase error by a factor of 4.6 for the same net GDD. With recent improvements in crystal technology, it is now possible to obtain high quality, highly doped (0.15%), short Ti:sapphire laser rods. Oscillators with such rods and silica prisms have produced pulses with durations as short as ~12-fs.[2, 4]

For common prism materials and operation at 800 nm, lowering the intracavity material paths will reduce but not eliminate cavity cubic phase errors. However at wavelengths longer than 800 nm the magnitude of the negative cubic phase contribution of prism pairs decreases relative to sapphire. It thus becomes possible at certain wavelengths for situations similar to that depicted for BeO in Fig. 3 to occur for more common materials.[19] The often made assumption that cavity cubic phase is minimized when intra-prism material is minimized is incorrect for prisms made of these materials at these wavelengths. In Fig 4, we show as a function of wavelength the magnitude of the cubic phase for a 1 cm sapphire rod and for prism pairs composed of eight optical materials in the limit of no intraprism path. The wavelength at which the prism and rod curves intersect is $\lambda_{0p}$. At this wavelength cavity cubic phase may be eliminated for zero prism insertion. As one inserts more prism into the beam this wavelength shifts. Figure 5 illustrates the range over which the cubic phase may be nulled for a given prism insertion. These values range from ~800 nm for BeO and ~850 nm for silica all the way to ~1040 nm for SF10. It should be noted that sub 100-fs pulse generation in Ti:sapphire has been demonstrated throughout this wavelength range, with pulses as short as 62 fs having been reported as far in the infrared as 1053 nm.[6] For $\lambda < 847$ nm, however, where the shortest pulses to date have been generated, we have found no commercially available prism material that will zero cubic phase. This situation is quite different for Cr:$LiSrAlF_6$. Figure 6 shows the prism material path length required for zero cubic phase in a zero GDD cavity

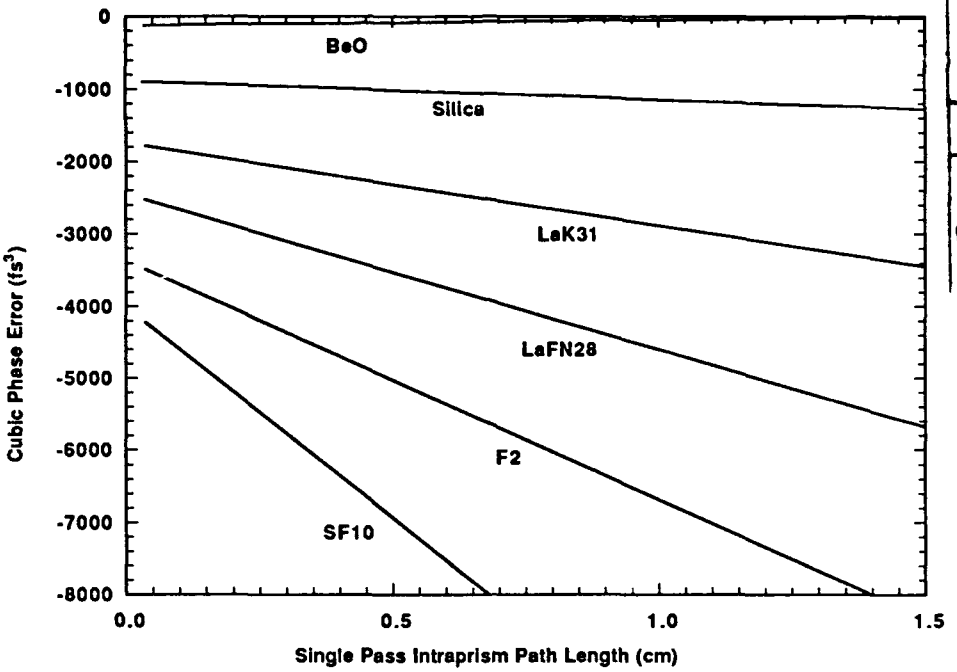


Figure 3. Round-trip cubic phase error versus the single-pass intraprism path length for a zero-GDD cavity containing a 2-cm e-sapphire rod.

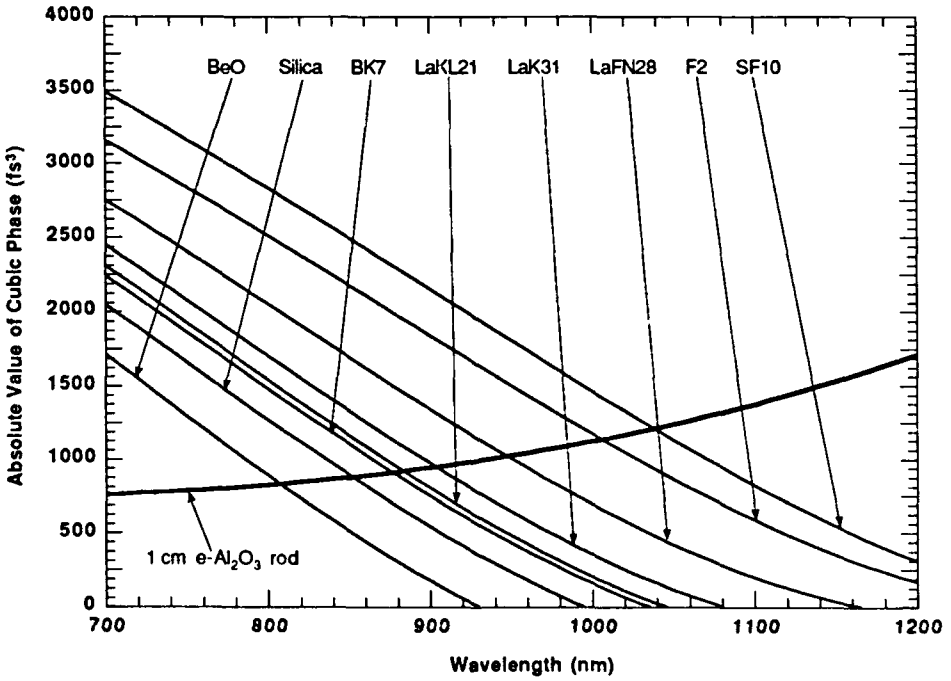


Figure 4. Magnitude of round-trip cubic phase for a 1-cm e-sapphire rod and various Brewster prism pairs. Zero round-trip cavity GDD and zero intraprism path length are assumed.

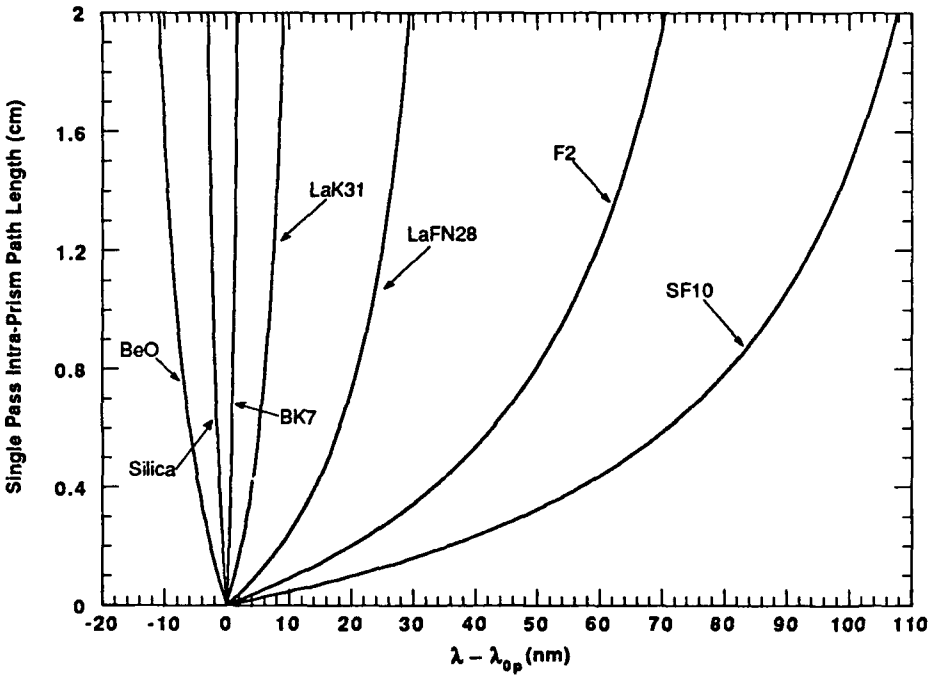


Figure 5. Intraprism path length as a function of wavelength relative to $\lambda_{0p}$, required to simultaneously null both GDD and cubic phase in a cavity consisting of a 1-cm Ti:sapphire rod and a Brewster prism pair.

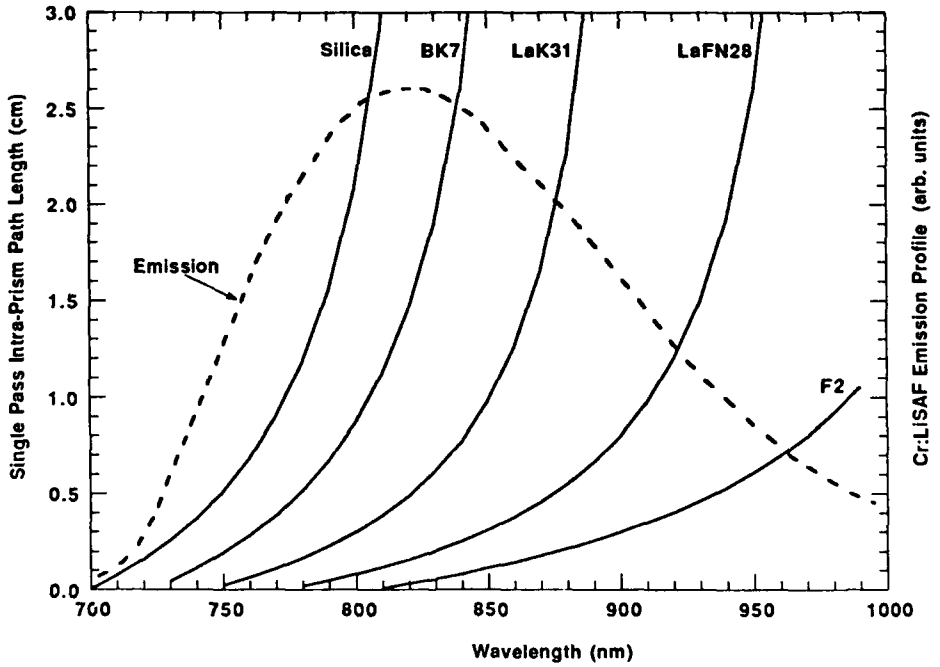


Figure 6. Intraprism path length required to null cubic phase as a function of wavelength, assuming Brewster prisms, zero round-trip cavity GDD, and a 2-cm Cr:LiSAF rod. The dashed curve is the emission profile of Cr:LiSAF.

containing a 2-cm Cr:LiSrAlF$_6$rod and Brewster prisms. Superimposed is the emission profile of Cr:LiSrAlF$_6$. As we can see from the figure, zero cubic phase can be easily obtained at any wavelength within the tuning range of Cr:LiSrAlF$_6$. In particular, at 825 nm, BK7 Brewster prisms with 2 cm of single pass intraprism path length will give zero cavity cubic phase. In general less dispersive laser materials such as Cr:LiSrAlF$_6$will result in shorter zero cubic phase wavelengths, $\lambda_{0p}$.

2.4 Increase of pulse spectral content

While the reduction of intracavity phase errors will allow shorter pulses to propagate without distortion, the duration of the pulse will also be determined by its spectral content. This content may be increased by increasing the amount of self-phase-modulation that occurs in the laser rod, which in turn is accomplished by increasing the intracavity pulse energy. Increasing the intracavity pulse energy may be accomplished by decreasing the cavity output coupling, however, this is most easily done by raising the pump power. Raising the pump power, however, changes the amount of thermal lensing and, to a lesser extent, self focusing, that occurs in the laser rod. This change can be compensated for without affecting intracavity alignment or dispersion by adjusting the translatable intracavity focusing mirror shown in Fig. 1. In this way, we can reproduce the far field cw profile of Fig. 2 (a) over a wide range of pump powers (between 7 and 20 watts). Mode locking then immediately ensues when the AOM is turned on. Figure 7 shows the increase of pulse spectral content and the corresponding decrease in pulse duration as we increase the intracavity power. The focusing mirror was translated 230 μm over the full range shown. The spectral structure which develops at higher powers is indicative of self phase modulation. It should be noted that at the highest powers the high modulation depth AOM not only initiates self-modelocking but also inhibits any concurrent cw mode operation.

Finally, it should be noted that in order for the most self-phase-modulation to occur, the intracavity pulse must not only have high energy but also have short duration at the laser rod. As will be explained in section 3, measurements of the pulse duration indicate that the pulse is transform limited at the doubling crystal of the autocorrelator. From this knowledge and measurements of the dispersive path encountered by the pulse, one may calculate the pulse duration at various locations in the laser cavity. In particular, for a pulse incident upon the laser rod from the direction of the intracavity prisms, the linear dispersive path includes the 2-cm Ti:sapphire rod (GDD = +1120 fs$^2$), the silica AOM (GDD = +430 fs$^2$), a BK7 output coupler (GDD = +230 fs$^2$ ), a double pass extracavity LaK31 prism pair (GDD = -2520 fs$^2$), and the BK7 beam splitter of the autocorrelator (GDD = +664 fs$^2$). The net GDD of this dispersive path is -75 fs$^2$ thus indicating that the pulses depicted in Fig. 7 are shortest near the intracavity prism end of the laser rod.

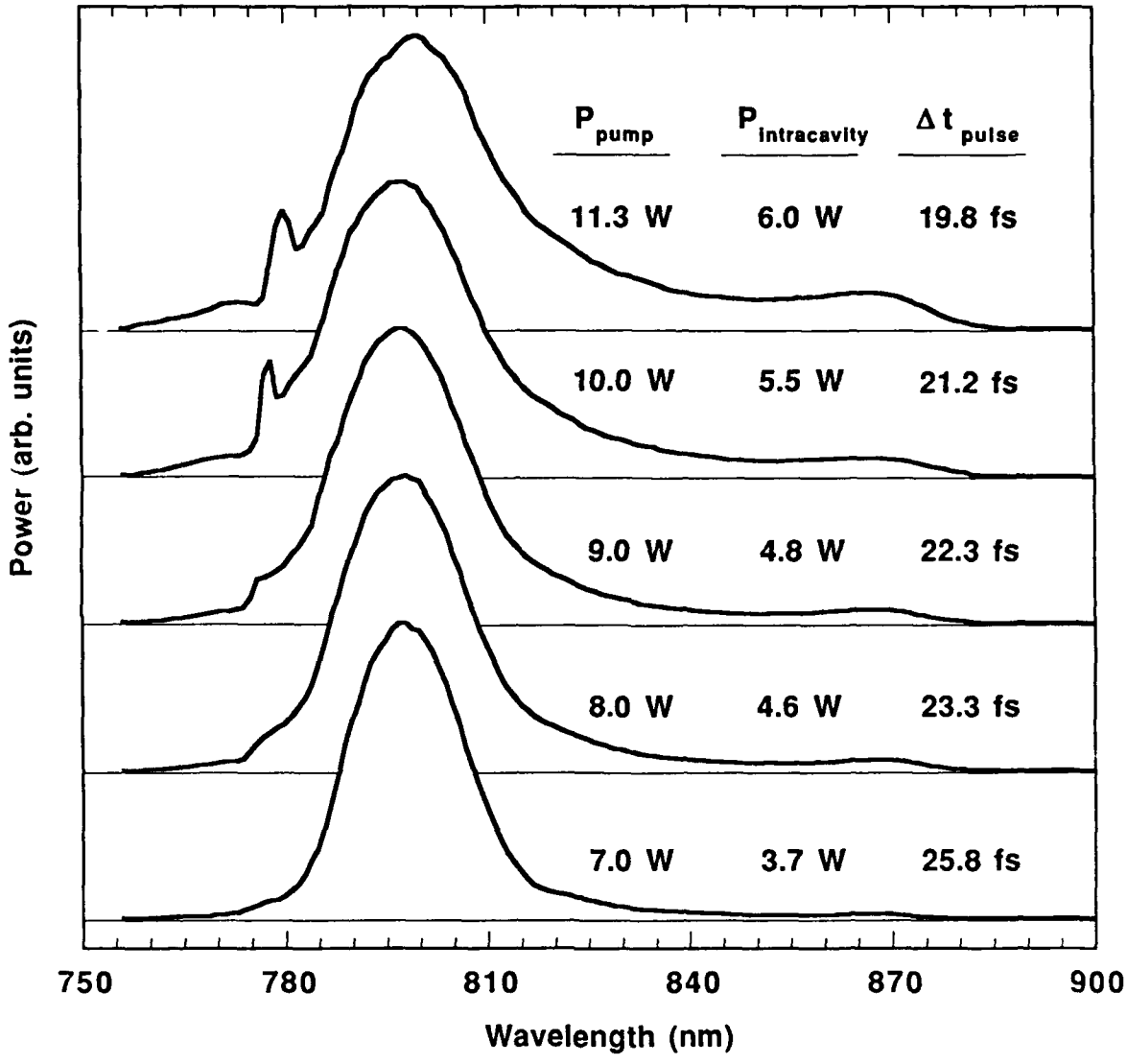


Figure 7. Pulse spectrum and pulse duration at five intracavity powers. The output coupling is 10%.

## 2.5 Bifurcation and double pulsing

Figure 7 suggests that we might further reduce the pulse duration by increasing the intracavity power beyond 6 W. However, at higher intracavity powers, the pulse bifurcates and two similar, slightly longer duration, lower energy pulses develop with a temporal separation that yields equal gain. The process by which a single pulse bifurcates at some critical intensity in the presence of positive dispersion may be explained by recent calculations of Rothenberg[23, 24]. With the AOM off, the two pulses separate by one-half the round trip time of the cavity. With the AOM on, this separation shortens to between 10 ps and 50 ps. The exact separation is stable but is dependent upon the phase and power of the rf driving the AOM. Such closely spaced double pulses cannot be resolved with common photodiodes. The separation is also too large to be seen in typical high resolution autocorrelations. To observe these pulses, the output of the laser was monitored with a 2-ps resolution streak camera (Hamamatsu Model c1587). Typical streak camera traces are shown in Fig. 8. The traces differ only in phase and power of the rf which drives the AOM. Although a quantitative study has not been conducted, it is believed that this mode of operation should provide a convenient method for producing electronically controllable, variable delay, collinear pulses. Autocorrelations of the individual pulses indicate a duration of ~22 fs with a total output power of ~2 Watts. Further indication of the bifurcation process is also occasionally evident in the spectra of the pulses. Just above the threshold for bifurcation and before the pulses have separated to yield maximum gain, the pulses will interfere. The result is a highly modulated pulse spectrum. Such spectra have been observed but not recorded.

Bifurcation limits the intracavity power and hence the peak power of the output pulses. However, by scaling to larger output coupling, one may obtain a higher output at the same intracavity power. Simple scaling implies that if one increases the output coupling from 10% to 15%, the pump power should increase from 11.3 W to ~16 W in order to produce the same intracavity pulse energy. Under these conditions, we observe 22-fs pulses with a peak power of 430 kW. At a slightly higher pump power, 19 W, we have obtained 21-fs, ~500 kW peak power pulses with an average output power of 1.05 W. Uncompensatable thermal focusing limits the output power in the latter case.

## 2.6 Other chirp modes

Besides the double pulse mode, it is also possible to occasionally operate the laser in a single pulse mode that is similar to that described in section 2.4. Pulses in this mode have nearly identical pulse spectra but an entirely different chirp. It is believed that this mode of operation is in direct competition with the bifurcation process and corresponds to a pulse with longer duration and thus lower peak power in the laser rod. As a comparison, the spectra of this anomalous chirp mode and the short pulse mode that corresponds to highest peak power in the laser rod are shown in Fig. 9. The anomalous chirp mode

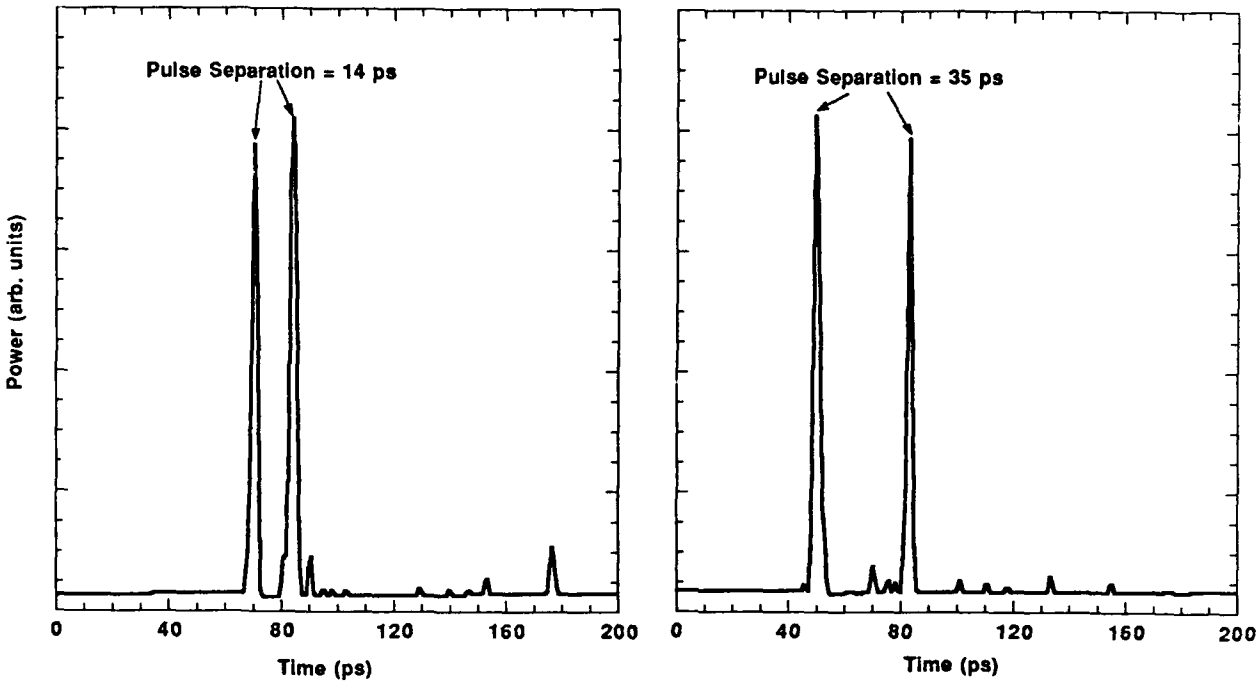


Figure 8. Typical streak camera traces for double pulse operation.

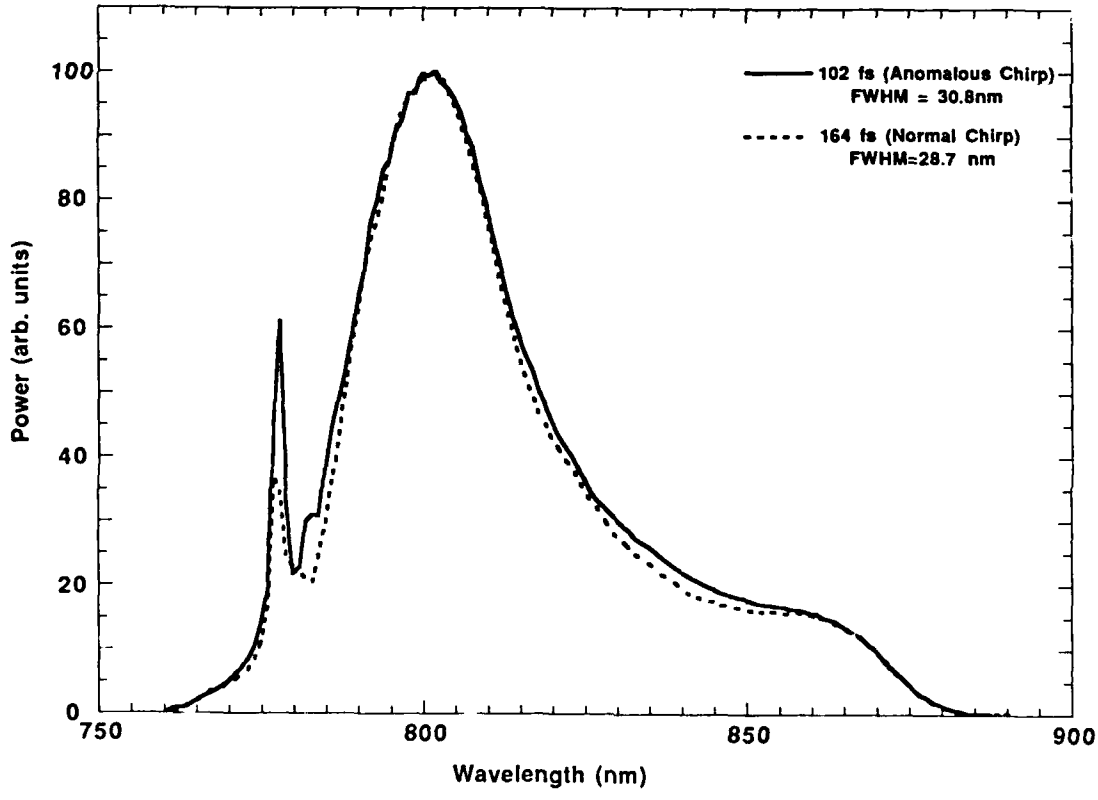


Figure 9. Comparison of spectra for normal and anomalous chirp modes.

requires an additional 911 $fs^2$ of positive GDD to produce a transform limited pulse at the doubling crystal of the autocorrelator. To illustrate this point we plot in Figs. 10 and 11 the calculated temporal form of the normal and anomalous pulses at the mirror surface of the output coupler. We calculate that this pulse is at its shortest as it leaves the laser rod on its way towards the AOM. The anomalous chirp mode only occurs at single pulse energies which correspond to the bifurcation limit or higher in the cavity.

## 3. MEASUREMENT OF ULTRASHORT PULSES

### 3.1 Fourier transform technique

The duration of ultrashort optical pulses must be determined indirectly. Typically one measures the full width at half maximum (FWHM) of the intensity autocorrelation and spectrum of the pulse. A "times transform limit" measure of the broadening of the pulse is obtained from the ratio of the measured FWHM time-bandwidth product and the theoretical time-bandwidth product corresponding to some assumed pulse shape. If this ratio is close to unity, then the pulse is said to be unchirped and the duration is "determined" by dividing the measured autocorrelation FWHM by the deconvolution factor of the assumed pulse shape. Tables of deconvolution factors for various pulse shapes and their autocorrelations exist in the literature.[25, 26] Although simple, this procedure is predicated on assumed knowledge of the pulse shape and is therefore flawed. The value of the time-bandwidth product is dependent upon the transform limited shape of the pulse and the amount of chirp present on the pulse. Different transform limited pulse shapes with different amounts of chirp may give the same time-bandwidth product. For ultrashort pulse lasers, it is commonly assumed that the envelope of the electric field of the pulse has a sech(t) time dependence. This shape satisfies simple models for mode-locked lasers in the presence of GDD compensation.[20, 21] However, for this assumption to be valid it is necessary that the spectrum of the pulse also correspond to the transform of sech(t) which is sech(ω). Clearly from Fig. 7 the short pulses that we obtain do not correspond to a $sech^2$ power spectrum since the spectra are not symmetric and not single peaked.

To avoid this problem, our determination of pulse duration combines a measurement of the full pulse spectrum and an interferometric autocorrelation with a numerical analysis that *makes no assumption of pulse shape*. Pulse spectra are measured with a 1 m scanning monochrometer (Spex Model 1704) and a calibrated silicon photodiode (Newport Model 835). The spectrum of a typical short pulse corrected for the response of the photodiode is shown in Fig. 12. To calculate the transform limited pulse shape, we simply Fourier transform the square root of the spectrum and square the result. This temporal shape is shown in the inset of Fig. 12 and has a FWHM of 20.2 fs. Any variation in phase between different spectral components will result in a longer duration pulse than that shown in Fig. 12. Once the transform limited temporal shape is calculated, we can numerically calculate its interferometric autocorrelation. We then measure the interferometric autocorrelation of the actual pulse and compare the two. A pair of LaK31

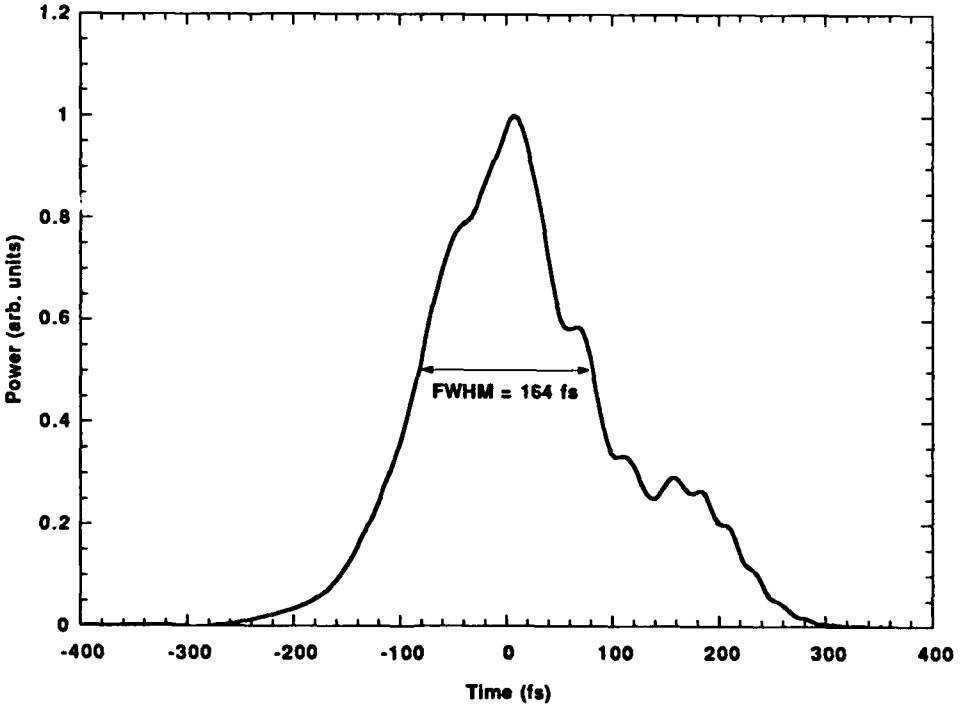


Figure 10. Temporal pulse shape of normal chirp mode at the reflective surface of the output coupler

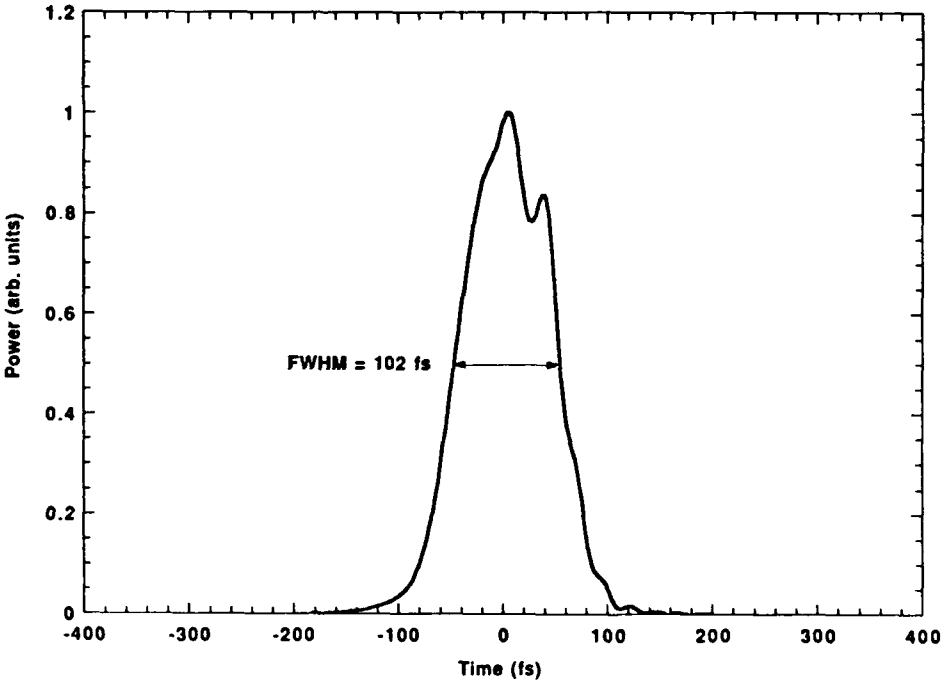


Figure 11. Temporal pulse shape of the anomalous chirp mode at the reflective surface of the output coupler

extracavity prisms is used to compensate for the GDD of the autocorrelator and to remove any other linear chirp present on the pulse. Because we use interferometric autocorrelation, we may monitor the degree of chirp on the pulse. As linear chirp is removed, all maxima in the lower envelope of the autocorrelation disappear.[26] The measured interferometric autocorrelation corresponding to the spectrum in Fig. 12, along with the HeNe interferogram used as a delay calibration, are shown in Fig. 13. Superimposed upon this autocorrelation is the calculated envelope of the interferometric autocorrelation of the transform limited pulse shape. The degree of agreement shown in Fig. 13 indicates that the actual pulse is within half a femtosecond of the transform limited pulse duration. For this particular case the measured average output power was 610 mW at a 100-MHz repetition rate, giving a peak power of ~ 300 kW.

Given the significant changes in spectral shape that we observe, it is necessary to repeat the above procedure for each autocorrelation. To illustrate this point we plot in Fig. 14 the calculated deconvolution factors that correspond to each of the spectra in Fig. 12. Such large changes in deconvolution factors can lead to situations in which longer duration autocorrelations actually correspond to shorter duration pulses.

The precision of the above technique is dependent upon accurate and complete measurement of the pulse spectrum. It is important not only to use calibrated measurement devices but also to measure the full spectral content of the laser pulse. Spectral components that are less than 1% of the peak intensity play an important role in producing a short pulse. To illustrate this point consider the following numerical experiment. We start with a 60-nm FWHM $sech^2$ power spectrum. Such a spectrum should correspond to a pulse of 11.27 fs in duration. However, this is only the case if we consider the pulse to have infinite frequency content. If instead, our 60-nm $sech^2$ spectrum is truncated to fit in a finite spectral window, then the corresponding pulse will be longer in duration. Such truncation could correspond to the finite bandwidth of the laser output coupler for instance. The resulting pulse duration as a function of the width of the spectral window is depicted in Fig. 15. Truncation at a width of ~200 nm corresponds to exclusion of all frequency components with amplitude less than 1 % of the peak. Such truncation would yield a pulse of only 13.6 fs in duration. It should be noted that typical single stack, broadband dielectric coated output couplers have bandwidths of approximately 200 nm.[27] This result clearly suggests that it is important to measure more than the FWHM of spectrum in order to accurately determine pulse duration. It also suggests that it should be difficult to obtain sub 10-fs $sech^2$ pulses with convensional optics.

3.2 Dispersion and loss balanced autocorrelator

In order to obtain an accurate autocorrelation of the pulse, it is important that the two pulses that are delayed with respect to one another at the doubling crystal of the autocorrelator be exact duplicates of each other. In order for this to be the case, it is necessary for the interferometer of the autocorrelator to not only have loss in each arm balanced but to also have dispersion in each arm balanced. This is not necessarily

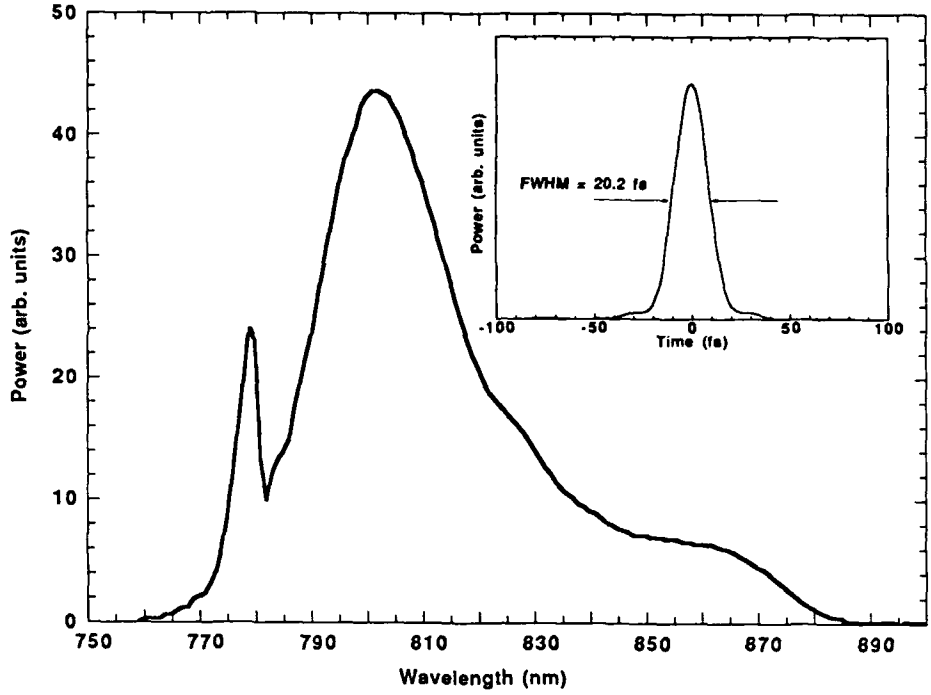


Figure 12. Power spectrum of a short pulse. Inset: Transform limited temporal profile (FWHM=20.2 fs) calculated from the spectrum.

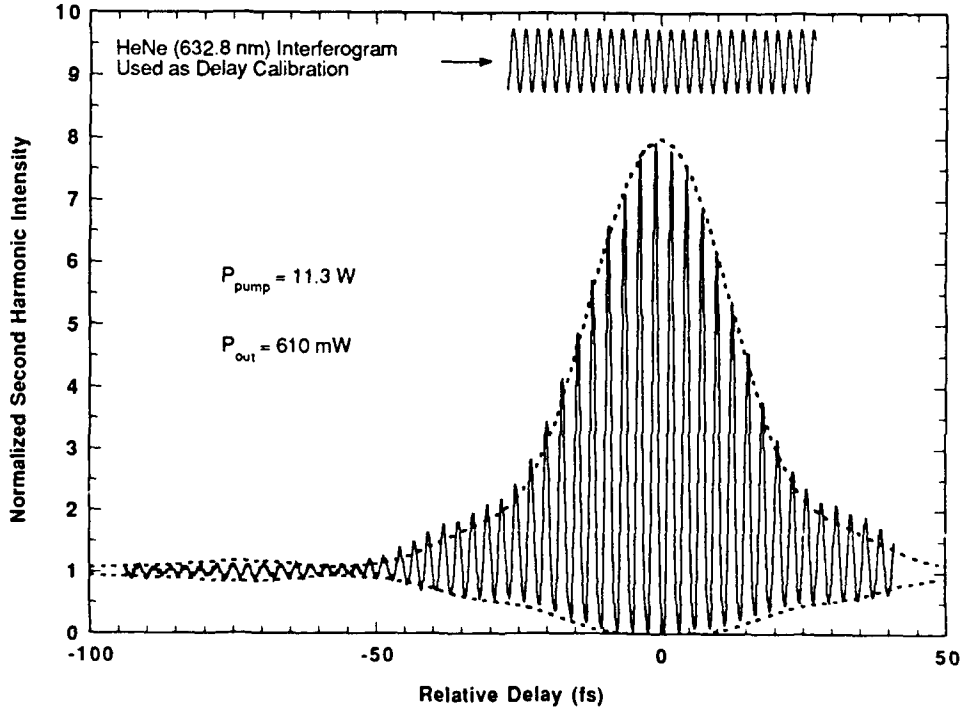


Figure 13. Measured interferometric autocorrelation of short pulse. Superimposed are the envelopes of the calculated interferometric autocorrelation of the transform limited 20-fs pulse from Fig. 12.

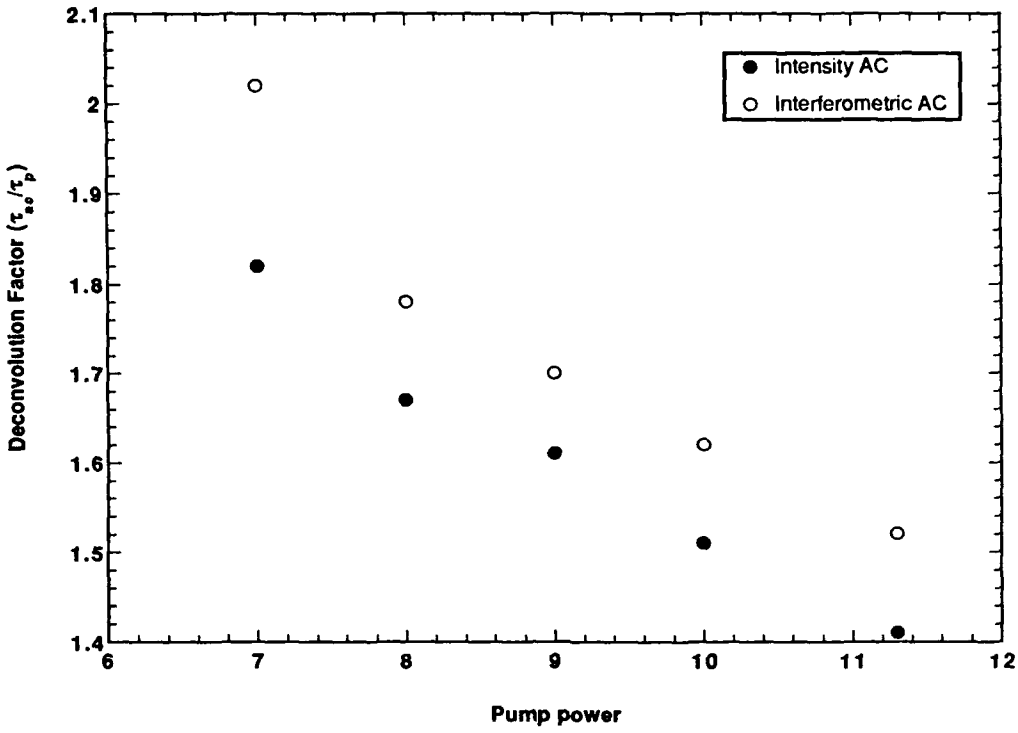


Figure 14. Intensity and interferometric deconvolution factors for spectra shown in Fig. 7.

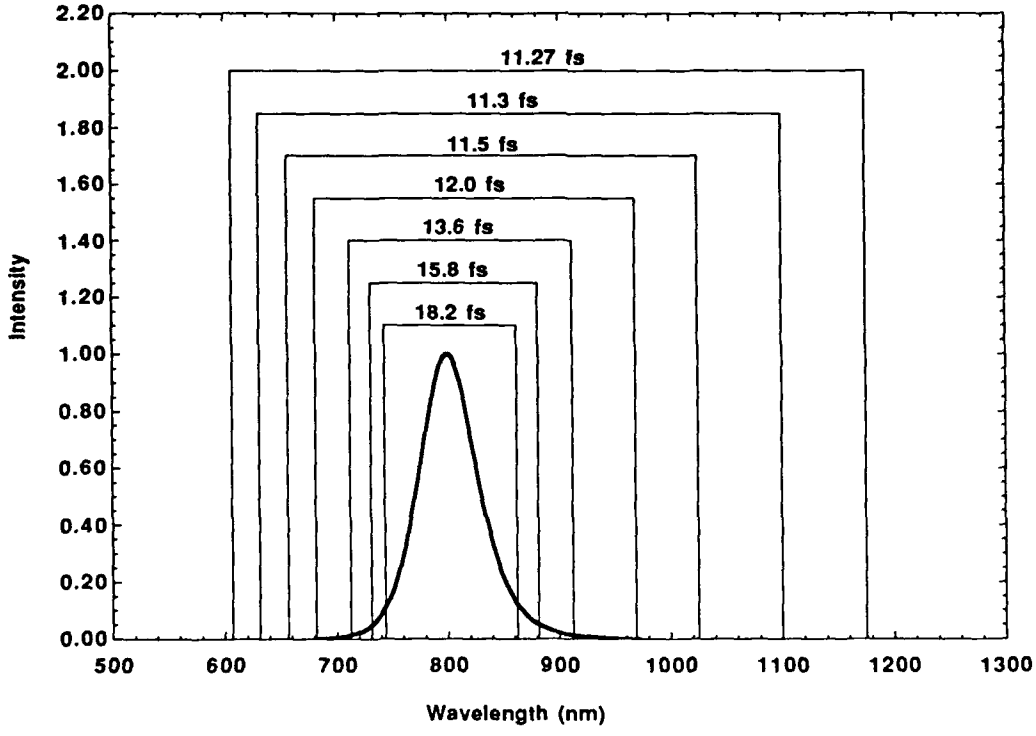


Figure 15. Variation of pulse duration for different spectral windows and a 60 nm FWHM $sech^2(t)$ pulse

the case for the typical Michelson interferometer used in most interferometric autocorrelators. Such an autocorrelator is depicted in Fig. 16. In this case, the pulse traversing the vertical arm of the interferometer passes through the beam splitter substrate twice while the pulse traversing the horizontal arm passes through the beam splitter only once. The two pulses when recombined will have different pulse durations. To circumvent this problem one may insert additional material, identical to the beam splitter substrate, into the horizontal arm. The path length of this material must be exactly half of the beam splitter thickness for the two pulses to see the same net dispersion. This new material, however, may introduce additional losses and therefore cause the recombined pulses to have different amplitudes. To avoid these difficulties, we use two identical beam splitters and two roof mirror assemblies to form an interferometer. This arrangement is depicted in Fig. 17. In this device, a pulse traveling through each arm traverses the beam splitter substrate only once and thus the durations of the recombined pulses are identical. Each pulse also experiences only one reflection and one transmission of the beam splitter coating and thus the amplitudes of the recombined pulses are also identical. A dispersive delay line consisting of LaK31 prisms is used prior to the interferometer to compensate for the dispersion of the beam splitters and any chirp on the pulse due to the laser oscillator. Dispersion in the harmonic generation crystal is minimized by using a thin (50 μm) KDP crystal.

There are some additional advantages to this arrangement shown in Fig. 17. Since roof mirror assemblies are used, there is no direct feedback of the optical signal to the laser source as in the Michelson arrangement. In addition there is more than one, non-overlapping optical path which may be used as an interferometer. This convenience can be used to simulataneously monitor the absolute displacement of one arm with respect to the other. In our case, this other path is occupied by a HeNe laser beam. In principal the interference fringes of the autocorrelation can be used to measure this displacement. However, as the bandwidth of the pulse becomes large, it becomes increasingly difficult to determine the exact carrier frequency of the pulse. With the HeNe interference pattern, it is possible to measure the absolute pulse delay of one arm with respect to the other to less than ~50 attoseconds.

### 3.3 Measurement limitations

The dominant "error" in the measurement device described above is higher order phase distortion. The prism delay sequence that is used prior to the autocorrelator will compensate for any linear chirp that may be present on the pulse and for the GDD of the autocorrelator. However, as stated earlier, higher order (cubic) phase distortions may also broaden the pulse. External to the laser cavity, these errors may be minimized by using a thinner output coupler, lower dispersion glass for the prism sequence and by using lower dispersion, thinner substrates for the autocorrelator beam splitters. In the present configuration, we estimate the cubic phase distortion due to these optics to be approximately -3800 $fs^3$. For the pulse shown in Fig. 12, this would result in a broadening of approximately 5 fs. For reasonable

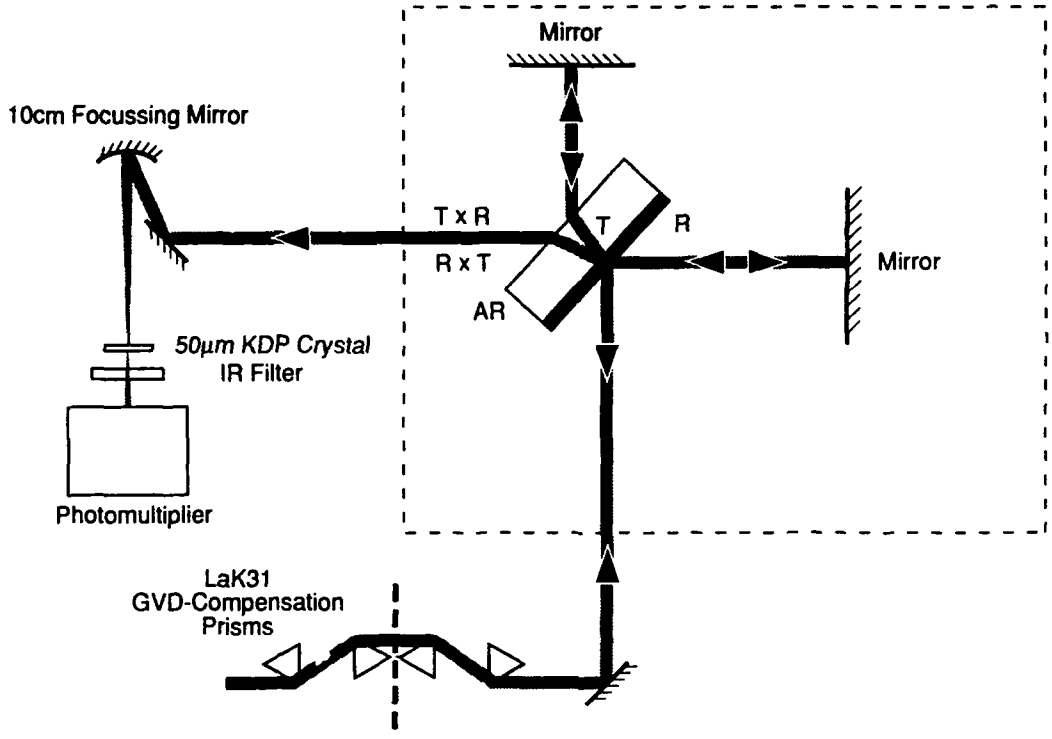


Figure 16. Schematic of Michelson interferometer based autocorrelator

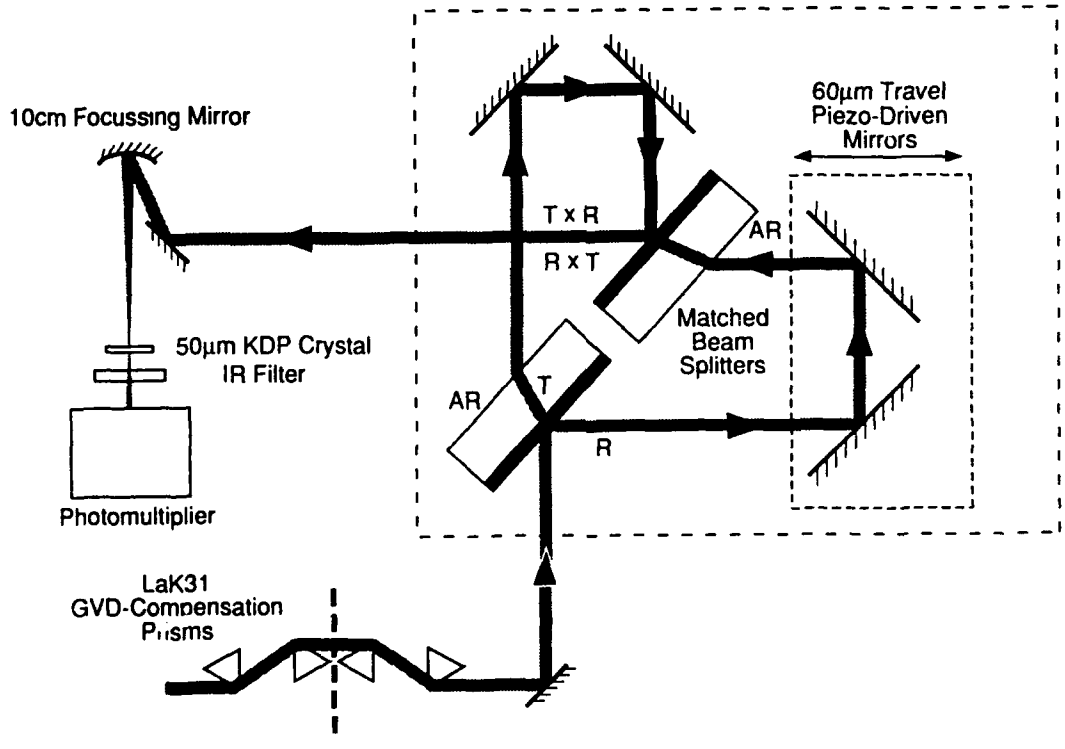


Figure 17. Schematic of GDD and loss matched interferometric autocorrelator

thicknesses and materials, it should be possible to reduce this cubic distortion to approximately -200 $fs^3$ or < 0.1 fs of broadening. However, one may not necessarily wish to eliminate this distortion. Indeed, since we measure a nearly transform limited pulse with our arrangement, the pulse exiting our laser has the opposite sign of cubic phase. In our case, negative cubic phase distortion is advantageous. In any respect, control and manipulation of higher order dispersion is necessary when measuring pulse durations of less 30 fs.

A less significant consideration is the frequency response of the autocorrelator. This response is limited by the dielectric coatings on the beam splitters. The amplitude modulation caused by the autocorrelator is the product of the transmission and reflectance of the coating. This product is significantly flatter than either component as illustrated in Fig. 18 and should cause negligible distortion of 10 to 20-fs pulses.

## 4. AMPLIFICATION CONSIDERATIONS

### 4.1 Chirped pulse amplification

Although many amplification systems now exist that are capable of producing terawatt, ~100-fs pulses[28, 29], the amplification of 20-fs pulses to similar levels will require significant design changes. These changes are necessary to avoid a variety linear and nonlinear pulse distortions which manifest themselves at short pulse durations. In particular, amplification systems based on chirped pulse amplification (CPA) will require new expander/compressor designs, elimination of refractive optics, and enclosure of compression stages in vacuum.

### 4.2 Quintic phase limited 10000 times expansion/compression

Key to all chirped pulse amplification systems is the ability to expand a seed pulse in time, amplify this long pulse and then recompress the amplified pulse to the original pulse duration. Traditional pulse expanders based on a pair of antiparallel gratings and a one-to-one refractive telescope[30] can produce pulse distortions due to frequency dependent material paths through the system. To avoid this problem we have designed and constructed a cylindrical mirror based pulse expander. Schematically this pulse expander is shown in Figure 19. In order to calculate the dispersive characteristics of this arrangement, including material in the amplification chain and the pulse compressor, we use a dispersive ray tracing analysis. This analysis includes the effects of finite beam size and divergence, both of which are significant on a 20-fs time scale. The beam traverses the system twice. On the first pass, a finite size beam experiences a spatially varying pulse expansion due to the mirror/grating asymmetry of the "z-fold" arrangement. This unwanted distortion, which can be be greater than the pulse duration, may be removed by inverting the beam in the horizontal plane with a four mirror arrangement before a second pass through the system. The

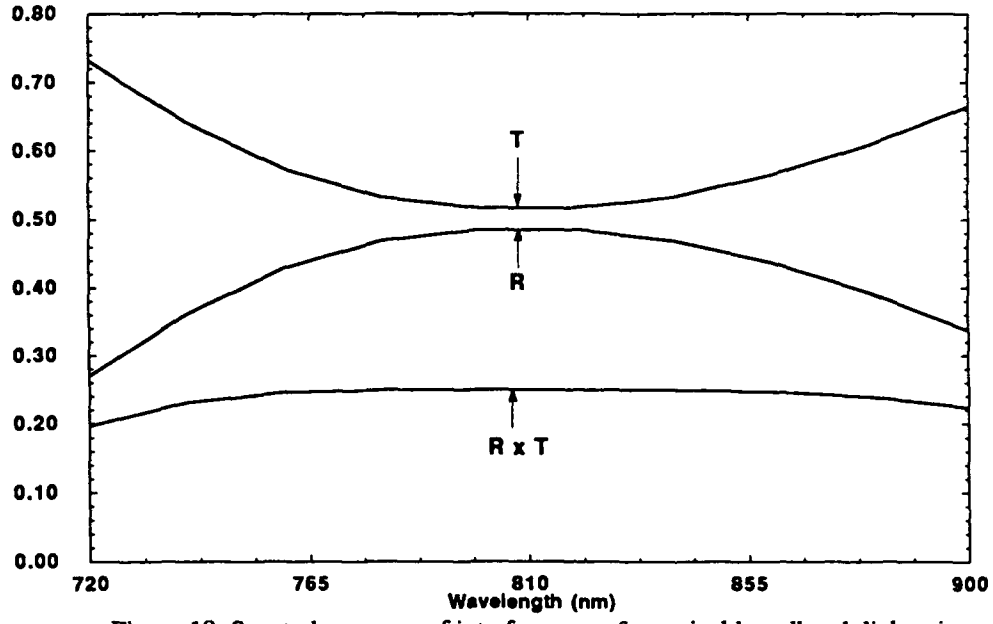


Figure 18. Spectral response of interferometer for typical broadband dielectric coated beamsplitter. Curves are for p-polarization.

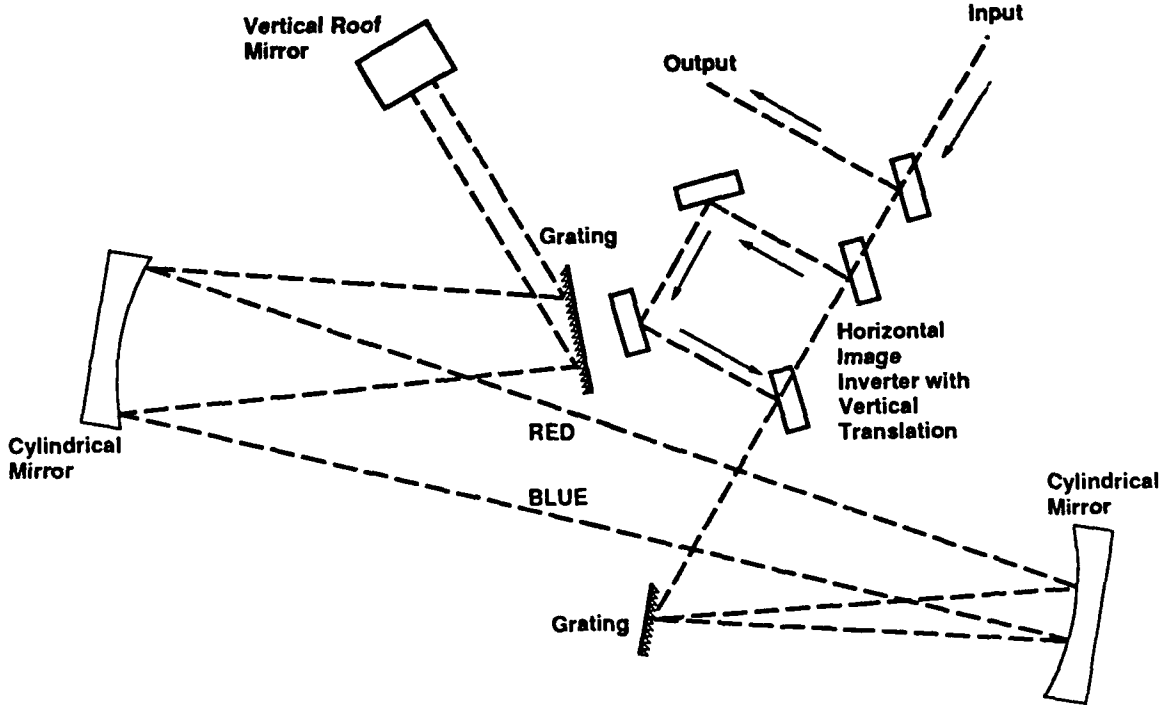


Figure 19. Schematic of a mirror based pulse expander. The beam path is multiplexed four times in the vertical dimension, with vertical translation occurring in the roof mirror and image inverter assemblies. In our implementation, the gratings are 1200 grooves/mm, and the mirrors are 100 cm radius of curvature.

result is a spatially uniform, expanded beam, which may be amplified and recompressed. It should be noted that the "z-fold", tangential focusing arrangement shown in Fig. 19 is unique in its ability to not produce significant pulse distortion. Other arrangements, i.e. "bow-tie" and/or sagittal focusing, each produce uncompensatable distortions. The degree to which one may recompress to the original pulse duration is dependent upon cancelation of frequency dependent phase shifts in the expander, amplifier and compressor. We show numerically that it is possible with correct choice of compressor grating angle and separation and correct amount of material path to cancel cubic and quartic phase distortion. Calculations indicate that it should be possible to expand 20-fs pulses by >10,000 times and recompress to within 1-fs of the original pulse duration. The final error being quintic phase limited.

4.3 Errors due to refractive optics

It is known that refractive optics, especially singlets, may lead to uncompensatable pulse distortions when used with ultrashort pulses.[31] This effect arises from the fact that different parallel input rays traverse different material paths in an optical system. This fact manifests itself in two ways. First, it leads to a delay of the chief ray with respect to the marginal ray, i.e. a curved pulse front. Second, it leads to a spatially varying pulse broadening. Both of these effects cannot be compensated for in a convenient manner. In order to calculate possible distortions due to amplifier beam expansion telescopes, we use a dispersive ray tracing analysis. The results of one such calculation are depicted in Fig. 20. In this plot, we present pulse delay as a function of input beam diameter for a 6.7 times magnification, Galilean telescope based on BK7 glass lenses. Also included in this plot is a paraxial analysis of the same telescope using the formulas of Bor.[31] As can be seen, the distortion for reasonable input beam diameters is on the order of our 20-fs pulse. This distortion leads to a longer effective pulse duration. It can also be seen from the figures that the ray tracing analysis predicts larger pulse front curvatures. This increased distortion is a result of spherical aberration. The effect of spatially varying dispersive broadening is shown in Fig. 21 for the same telescope. This effect is less significant. In order to avoid both effects we have constructed reflective telescopes based on cylindrical optics. Due to the relatively large diameter of our input beams to these telescopes, each dimension may be expanded sequentially without introduction of significant astigmatism.

4.4 Nonlinear distortion after compression

The current amplifier design should allow the production of 5-TW pulses (125 mJ in 25 fs) at a 10-Hz repetition rate. In this design, the final beam diameter will be 23 mm. This implies an unfocused intensity of $1.2 \times 10^{12}$ W/cm$^2$ after pulse compression. At these intensities, self-phase-modulation in air (nonlinear index = $6.3 \times 10^{-19}$ cm$^2$/W) is sufficient to cause a pi phase shift in ~0.5 meters. Self-phase-

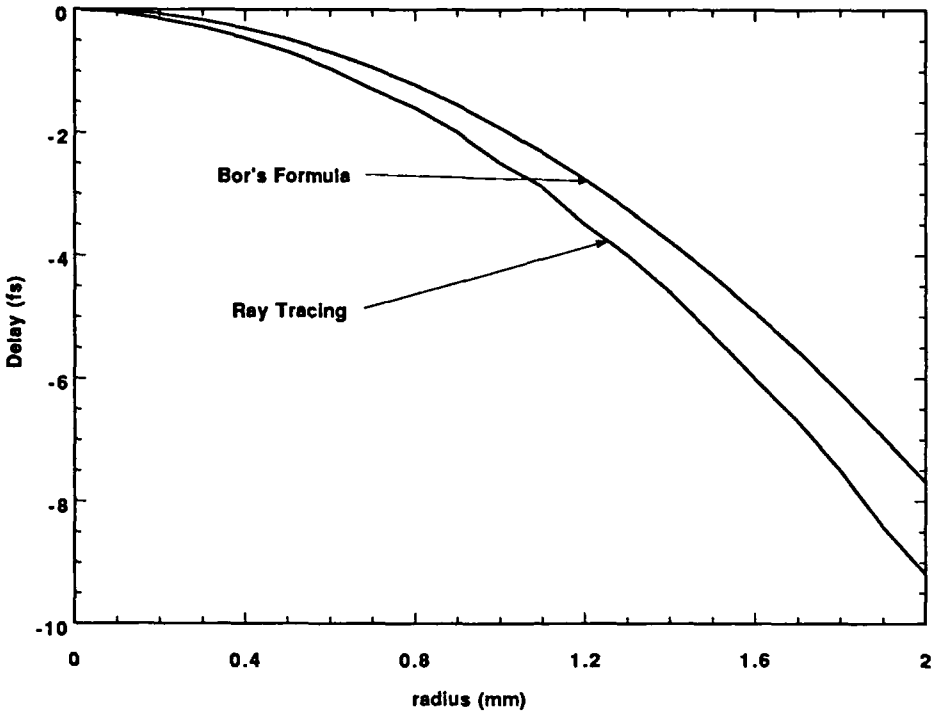

Figure 20. Delay versus radius for 6.7X BK7 Galilean telescope

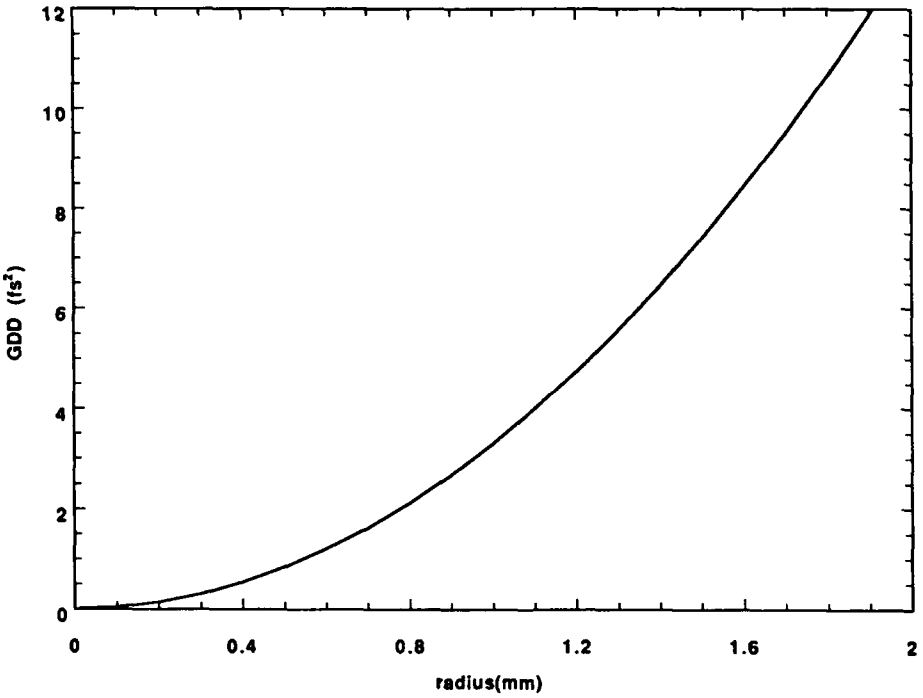

Figure 21. GDD versus beam radius for a 6.7X BK7 Galilean telescope

modulation in vacuum window materials would also be of the same magnitude. In order to avoid these distortions, it is necessary to place the compression stage and experiments in vacuum chambers.

## 5. CONCLUSIONS

General considerations necessary to produce, measure and amplify pulses with durations of 20-fs and shorter have been outlined. We have used a combination of cubic phase minimization and increased self-phase-modulation in a laser cavity to generate high peak power 20-fs pulses. We have found that a high-modulation-depth AOM allows us to run at higher intracavity energies than otherwise possible. We have clearly shown the effect of self-focusing on the spatial mode of the cavity and have demonstrated that increasing intracavity energy can decrease the pulse duration. We believe that extending these principles to future cavity designs with shorter laser rods, silica prisms, and high intracavity energies may result in the production of pulses of less than 10 fs in duration. In addition we have describe a measurement technique and autocorrelator that allow accurate determination of pulse duration and pulse shape. A quintic-phase-limited amplification system based on chirped pulse amplification and reflective optics has been described and should allow the production of 25-fs, 125-mJ, 5-TW pulses at a 10-Hz repetition rate.

## 6. ACKNOWLEDGMENTS

The work described here was supported by the Air Force Office of Scientific Research, the Army Research Office, the Strategic Defense Initiative Organization, the Office of Naval Research and through generous equipment loans from the Lawernce Livermore National Laboratory. B. E. Lemoff acknowledges the support of a National Science Foundation graduate fellowship.

## 7. REFERENCES

1. B. E. Lemoff and C. P. J. Barty, "Generation of high-peak-power 20-fs pulses from a regeneratively initiated, self-mode-locked Ti:sapphire laser," Optics Letters, **17**, 19, 1367-1369, 1992.

2. P. F. Curley, Ch. Spielmann, T. Brabec, F. Krausz, E. Wintner and A. J. Schmidt, "Operation of a femtosecond Ti:sapphire solitary laser in the vicinity of zero group-delay dispersion," Optics Letters, **18**, 1, 54-56, 1993.

3. B. Proctor and F. Wise, "Quartz prism sequence for reduction of cubic phase in a mode-locked Ti:$Al_2O_3$ laser," Optics Letters, **17**, 18, 1295-1297, 1992.

4. C.-P. Huang, M. T. Asaki, S. Backus, M. M. Murnane, H. C. Kapteyn and H. Nathel, "17-fs pulses from a self-mode-locked Ti:sapphire laser," Optics Letters, **17**, 18, 1289-1291, 1992.

5. J. M. Jacobson, K. Naganuma, H. A. Haus, J. G. Fujimoto and A. G. Jacobson, "Femtosecond pulse generation in a Ti:$Al_2O_3$ laser by using second- and third-order intracavity dispersion," Optics Letters, **17**, 22, 1608-1610, 1992.

6. J. D. Kafka, M. L. Watts and J.-W. J. Pieterse, "Picosecond and femtosecond pulse generation in a regeneratively mode-locked Ti:sapphire laser," IEEE Journal of Quantum Electronics, **28**, 10, 2151-2162, 1992.

7. K. Naganuma and K. Mogi, "50-fs pulse generation directly from a colliding-pulse mode-locked Ti:sapphire laser using an antiresonant ring mirror," Optics Letters, **16**, 10. 738-740, 1991.

8. N. H. Rizvi, P. M. W. French and J. R. Taylor, "Continuously self-mode-locked Ti:sapphire laser that produces sub-50-fs pulses," Optics Letters, **17**, 4, 279-281, 1992.

9. N. Sarukura, Y. Ishida and H. Nakano, "Generation of 50-fs pulses from a pulse-compressed, cw, passively mode-locked Ti:sapphire laser," Optics Letters, **16**, 3, 153-155, 1991.

10. D. E. Spence, P. N. Kean and W. Sibbett, "60-fsec pulse generation from a self-mode-locked Ti:sapphire laser," Optics Letters, **16**, 1, 42-44, 1991.

11. J. M. Evans, D. E. Spence, W. Sibbett, B. H. T. Chai and A. Miller, "50-fs pulse generation from a self-mode-locked Cr:LiSrAlF$_6$ laser," Optics Letters, **17**, 20, 1447-1449, 1992.

12. N. H. Rizvi, P. M. W. French and J. R. Taylor, "Generation of 33-fs pulses form a passively mode-locked $Cr^{3+}$:LiSrAlF$_6$ laser," Optics Letters, **17**, 22, 1605-1607, 1992.

13. P. Maine, D. Strickland, P. Bado, M. Pessot and G. Mourou, "Generation of ultrahigh peak power pulses by chirped pulse amplification," IEEE Journal of Quantum Electronics, **24**, 2, 398-403, 1988.

14. T. Brabec, C. Spielmann, P. F. Curley and F. Krausz, "Kerr lens mode locking," Optics Letters, **17**, 18, 1292-1294, 1992.

15. J. D. Kafka, M. L. Watts and T. Baer, "High-power regenerative mode-locking of a Ti:sapphire laser," Digest of Conference on Lasers and Electro-Optics, paper JMB3, Optical Society of America, Washington, D. C., 1991.

16. D. E. Spence, J. M. Evans, W. E. Sleat and W. Sibbett, "Regeneratively initiated self-mode-locked Ti:sapphire laser," Optics Letters, **16**, 22, 1762-1764, 1991.

17. C.-P. Huang, H. C. Kapteyn, J. W. McIntosh and M. M. Murnane, "Generation of transform-limited 32-fs pulses from a self-mode-locked Ti:sapphire laser," Optics Letters, **17**, 2, 139-141, 1992.

18. F. Krausz, Ch. Spielmann, T. Brabec, E. Wintner and A. J. Schmidt, "Generation of 33-fs optical pulses from a solid-state laser," Optics Letters, **17**, 3, 204-206, 1992.

19. B. E. Lemoff and C. P. J. Barty, "Cubic-phase-free dispersion compensation in solid-state ultrashort-pulse lasers," Optics Letters, **18**, 1, 57-59, 1993.

20. F. Krausz, M. E. Fermann, T. Brabec, P. F. Curley, M. Hofer, M. H. Ober, Ch. Spielmann, E. Wintner and A. J. Schmidt, "Femtosecond solid state lasers," IEEE Journal of Quantum Electronics, **28**, 10, 2097-2122, 1992.

21. H. A. Haus, J. D. Moores and L. E. Nelson, "Effect of third-order dispersion on passive mode locking," Optics Letters, **18**, 1, 51-53, 1993.

22. M. J. Weber, ed., CRC Handbook of Laser Science and Technology, Vol. 3, 193, CRC Press, Boca Raton, Fla., 1986.

23. J. E. Rothenberg, "Pulse splitting during self-focusing in normally dispersive media," Optics Letters, **17**, 8, 583-585, 1992.

24. J. E. Rothenberg, "Space-time focusing: breakdown of the slowly varying envelope approximation in the self-focusing of femtosecond pulses," Optics Letters, **17**, 19, 1340-1342, 1992.

25. K. L. Sala, G. A. Kenney-Wallace and G. E. Hall, "CW autocorrelation measurements of Picosecond Laser Pulses," IEEE Journal of Quantum Electronics, **16**, 9, 990-996, 1980.

26. J.-C. M. Diels, J. J. Fontaine, I. C. McMichael and F. Simoni, "Control and measurement of ultrashort pulse shapes (in amplitude and phase) with femtosecond accuracy," Applied Optics, **24**, 9, 1270-1281, 1985.

27. A. G. Jacobson, CVI Laser Corporation, private communication.

28. J. D. Kmetec, J. J. Macklin and J. F. Young, "0.5-TW, 125-fs Ti:sapphire laser," Optics Letters, **16**, 13, 1001-1003, 1991.

29. A. Sullivan, H. Hamster, H. C. Kapteyn, S. Gordon, W. White, H. Nathel, R. J. Blair and R. W. Falcone, "Multiterawatt 100-fs laser," Optics Letters, **16**, 18, 1406-1408, 1991.

30. O. E. Martinez, "3000 times grating compressor with positive group velocity dispersion: application to fiber compensation in 1.3-1.6 μm region," IEEE Journal of Quantum Electronics, **23**, 1, 59-64, 1987.

31. Z. Bor, "Distortion of femtosecond laser pulses in lenses and lens systems," Journal of Modern Optics, **35**, 12, 1907-1918, 1988.